



Repositorio Institucional de la Universidad Autónoma de Madrid

<https://repositorio.uam.es>

Esta es la **versión de autor** del artículo publicado en:
This is an **author produced version** of a paper published in:

CrystEngComm 21.20 (2019): 3232-3239

DOI: <https://doi.org/10.1039/c9ce00313d>

Copyright: © The Royal Society of Chemistry 2019

El acceso a la versión del editor puede requerir la suscripción del
recurso Access to the published version may require subscription

Reversible transformation between Cu(I)-thiophenolate coordination polymers displaying luminescence and electrical properties

Javier Troyano,^a Óscar Castillo,^b Pilar Amo-Ochoa,^{a,c} J. Ignacio Martínez,^d Félix Zamora,^{*,a,c,e} and Salomé Delgado^{*,a,c}

One-dimensional $[\text{Cu}_6\text{I}_3(\text{TP})_3(\text{MeCN})_2]_n$ (**1**) coordination polymer (CP) has been prepared by direct reaction between CuI and thiophenol ligand (TP). Reversible conversion reaction between **1** and the homoleptic 1D-CP $[\text{Cu}(\text{TP})]_n$ (**2**) is observed in acetonitrile upon controlling the CuI ratio. Interestingly, CPs **1** and **2** are multifunctional materials showing both luminescence and electrical properties. Photoluminescence measurements reveal that **1** and **2** are emissive in the blue and the red region, respectively. Additionally, both materials show electrical conductivity at room temperature (1.2×10^{-8} for **1** and 3.7×10^{-4} S cm^{-1} for **2**) indicating a semiconductor behaviour. DFT calculations have been used to rationalise these observations.

Introduction

In recent years, Cu(I) coordination polymers have received much attention in the material science, due to not only their fascinating architectures and intriguing topologies, but also for their interesting electronic properties.¹⁻⁴ Due to their high efficiency and low cost, copper(I) complexes have been extensively studied for their potential application in electroluminescent devices.⁵⁻¹¹

Copper(I) halide aggregates represent a versatile family in coordination chemistry because of their enormous structural diversity.¹² These aggregates could exist as discrete compounds or as CuX-based clusters forming coordination polymers. In general, the crystal engineering of copper halides is a challenge, due to the lack of understanding of the crystallisation process, where the aggregates transform from the solution phase to the crystal phase undergoing constitutional or conformational changes.¹³ This way, variations in the crystallisation conditions, such as solvent, temperature, concentration, might be responsible for variations in the composition and structure of the CuX-based complexes.¹⁴⁻¹⁹ Typically, copper(I) halide based

coordination polymers are constructed from neutral ligands such as anilines, pyridyl type ligands, thioethers and phosphines that connect the CuX aggregates.^{12, 20-24} Although the chemistry of copper(I) thiolate compounds has been explored, since the pioneering works of Coucouvanis and Harvey isolating $[\text{Cu}_4(\text{SC}_6\text{H}_5)_6]^{2-}$ cluster²⁵ or mixed-valence copper-mercaptide species²⁶ respectively, neutral Cu(I) thiolate coordination polymers $[\text{Cu}(\text{SR})]_n$ have been less investigated.²⁷ Nevertheless, the use of anionic thiolates with flexible coordination ability can also provide CPs based on Cu(I)-halides. It was found that the bridging ligand (connecting the copper halide aggregates) gave rise to more complicated architectures than did monodentate or bidentate chelating ligands. Thiolates may act both as terminal or bridging ligands with flexible coordination ability, and its reaction with copper(I) halides may produce compounds with new and intriguing structures. Furthermore, the interaction of “soft” sulfur atoms with “soft” Cu(I) ions may lead to enhance electronic communication between the ligand and metal centres, since the orbital energies are better matched.^{28, 29} In fact, it has been observed that the incorporation of organosulfur bridging ligands between adjacent transition metals is highly desirable to produce electrical conductive materials³⁰⁻³⁴ and previous studies by our group showed that CPs constructed from phenylthiolate ligands and copper(I) may exhibit thermochromic luminescence and semiconductor behaviour,^{35,36} what makes these compounds with high potential as multifunctional materials.

In this work we have investigated the self-assembly of CuI with thiophenol (TP), which has allowed us to isolate a novel 1D coordination polymer $[\text{Cu}_6\text{I}_3(\text{TP})_3(\text{MeCN})_2]_n$ (**1**). This compound was shown to undergo a reversible conversion into previously reported $[\text{Cu}(\text{TP})]_n$ (**2**).³² Here we describe the synthesis, structure, thermal stability, photoluminescent and electrical

^a Departamento de Química Inorgánica, Universidad Autónoma de Madrid, 28049 Madrid, Spain.

^b Departamento de Química Inorgánica, Universidad del País Vasco, UPV/EHU, Apartado 644, E-48080 Bilbao, Spain.

^c Institute for Advanced Research in Chemical Sciences (IAdChem) Universidad Autónoma de Madrid, 28049 Madrid, Spain.

^d Departamento de Nanoestructuras, Superficies, Recubrimientos y Astrofísica Molecular, Instituto de Ciencia de Materiales de Madrid (ICMM-CSIC), 28049 Madrid, Spain.

^e Instituto Madrileño de Estudios Avanzados en Nanociencia (IMDEA Nanociencia), Cantoblanco, 28049 Madrid, Spain.

Electronic Supplementary Information (ESI) available including additional structural and characterization data. File in CIF format for compounds **1** and **2** [CCDC 1504677-1504680]. See DOI: 10.1039/x0xx00000x

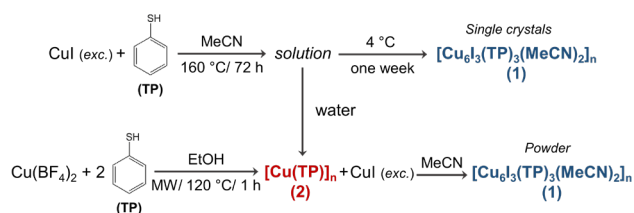
properties of both 1D Cu(I)-thiophenolate CPs, showing that can be used as multifunctional materials.

Results and discussion

Synthesis and Reversible Transformation Studies

The synthetic route to Cu(I)-thiophenolate coordination polymers **1** and **2** is given in Scheme 1. The reaction between CuI and thiophenol was investigated under solvothermal conditions. Thus, a mixture of CuI and TP (4:1 molar ratio) in acetonitrile was heated at 160 °C for 72 h. Then, the mixture was filtered off to separate the unreacted CuI and the resulting yellow solution was allowed to stand in a refrigerator. After one week, few single crystals of **1** were formed. In order to produce bulk sample for further measurements, we attempted to obtain **1** by anti-solvent precipitation with distilled water. The resulting yellow precipitate was characterized through XRPD. Unexpectedly, the obtained pattern did not match that of compound **1**. Instead, XRPD pattern corresponded to previously reported polymer **2**.³² Such observations led us to study the conditions in which the formation of these two compounds take place. Initially, we evaluated the possibility to produce compound **1** by reacting **2** and CuI. To this end, **2** powder was exposed to acetonitrile CuI solutions, ranging from 0 to 4 equivalents, at room temperature for 24 h, and the products were characterized by XRPD (Figure 1a). A comparison of the resulting patterns revealed that **2** undergo a conversion into **1** when at least two equivalents of CuI are used. However, the formation of **1** as a pure phase only occurs at four equivalents of CuI. By following this method, bulk synthesis of **1** as pure polycrystalline solid was achieved (see experimental section). Next, we investigated the reversibility of this transformation by exposing **1** to acetonitrile CuI solutions by following the same procedure described for **2**. Figure 1b shows the XRPD patterns of the products obtained indicating that compound remains invariable when CuI is in solution. However, when **1** was suspended in acetonitrile the formation of **2** was observed. These results point out the existing equilibrium between **1** and **2** in acetonitrile when CuI is added (Figure 1c). Thus, the formation of **1** can be achieved by increasing the concentration of CuI in acetonitrile suspensions of **2**, but when the ratio of CuI decreases, **1** reverts to compound **2**.

Besides the fact that coordination polymers are often described as “insoluble”,^{37, 38} it has been shown that these compounds may undergo solvent-mediated transformations.^{39–45} These processes involve dissolution of the initial coordination



Scheme 1 Synthetic routes of compounds **1** and **2**.

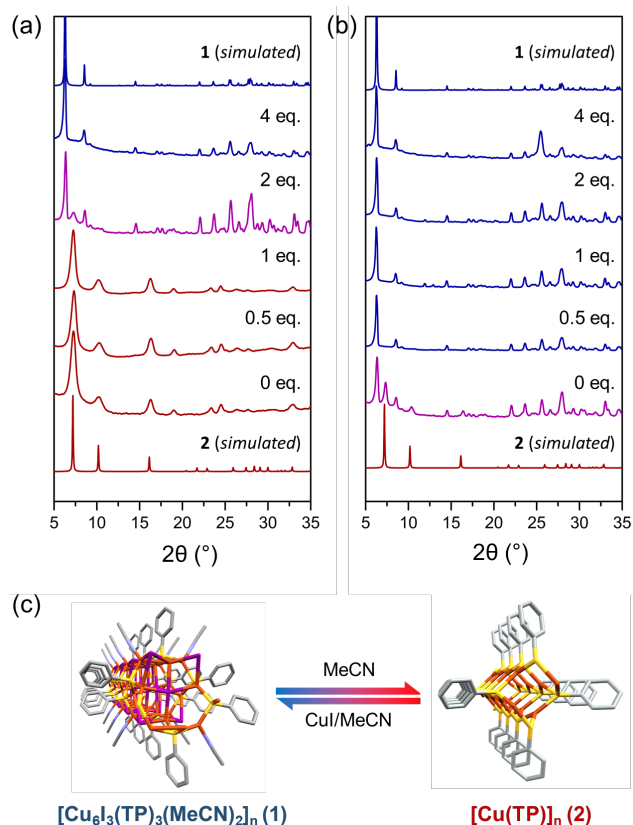


Fig. 1. XRPD patterns of the products obtained after exposing **2** (a) and **1** (b) to CuI solutions (0 to 4 equivalents) in MeCN for 24 h at room temperature, indicating the equilibrium between **1** and **2** species in CuI solutions in acetonitrile (c).

polymer, followed by the formation of a new phase from the solution. Otherwise, the solubility of coordination polymers depends strongly on the physical properties of the solvent and on its ability to bind metal cations constituting the backbone of the coordination polymer. In the case of Cu(I) based CPs, acetonitrile can stabilize the copper(I) species in solution due to its coordination ability. We have reported that Cu(I)-halide/thioacetamide CPs have the capability of reversibly disassembling in their building units and reassembling in acetonitrile.⁴⁶ Furthermore, we have also studied the transformations in acetonitrile of Cu(I)-halide mixed ligand compounds based on thioacetamide and *N,N'*-ditopic ligands, such as 4,4'-bipyridine and pyrazine,³⁶ showing that can lose one type of ligand (S- or N-donor ligand) and form new species with different ligand composition. In our case, acetonitrile seems to play a key role in the assembly-disassembly process, allowing the solubilization of the building blocks. Then the interconversion between compounds **1** and **2** depends on the ratio between thiophenolate ligand and CuI, where the formation of **1** is only favoured when an excess of CuI is present.

Thermal Analysis

Thermal gravimetric analysis (TGA) was performed on polymer **1** by heating the compound up to 700 °C in N₂ atmosphere (Figure S1). The obtained pattern shows the removal of the acetonitrile molecules between 60 and 103 °C with a mass loss of 6.7 % (calculated 7.0 %). The loss of acetonitrile was confirmed by heating **1** at 140 °C under N₂ atmosphere. The FT-IR spectrum of the resulting powder showed the disappearance of the bands at 2305 and 2272 cm⁻¹, and the band at 2920 cm⁻¹, due to nitrile and methyl groups, respectively (Figure S2). Further mass loss of 31.4 % is observed between 247 and 348 °C. This step can be assigned to the decomposition of thiophenolate ligand by cleavage of the carbon-sulfur bond, that has been previously observed for **2** and other polymeric copper(I) arylthiolates.^{32, 35, 47} Calculations indicate that the decomposition product is a mixture of CuI and Cu₂S (calculated 30.9 %).

Crystal Structures

The crystal structure of compound **1** shows some similarities with the previously reported compound **2** such as the 1D nature of the resulting coordination network and the presence of fused Cu_xS_x rings (Figures 2 and 3). However, the crystal structure of compound **1** is far more complex than the quite regular one of compound **2**. In compound **2**, it is based on Cu₃S₃ non planar rings that are fused together to generate a 1D nanotubular structure with a square section of 3.51 Å edges. Each copper(I) metal centre is coordinated to three sulphur atoms from the thiophenolate ligands to provide a planar triangular coordination geometry and each thiophenolate ligand bridges three copper(I) atoms through its sulphur atom (Figure 3). As previously stated, the crystal structure of compound **1** although showing the same 1D nature is more complex as the presence of bridging iodide anions and acetonitrile terminal

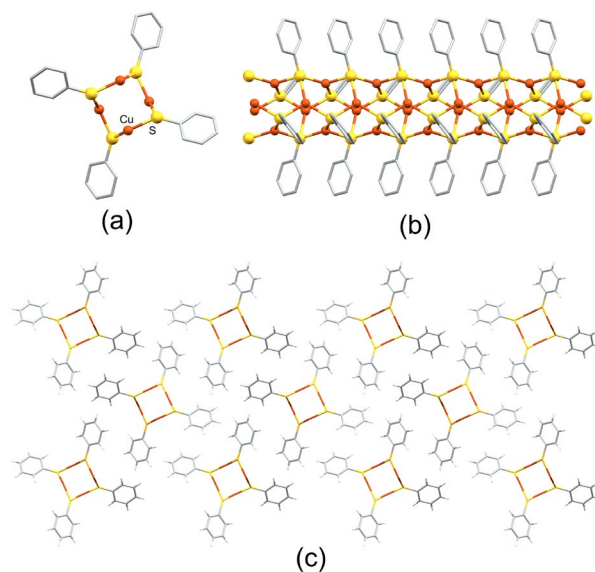


Fig. 3. View (a) along and (b) running along the *c*-axis of the 1D [Cu(TP)]_n (**2**) chains and (c) their crystal packing.

ligands generates a greater variety of the coordination surroundings for the copper(I) metal centres. In fact, crystallography independent six metal centres, three iodides, three thiophenolate and two acetonitrile ligands are distinguishable. Three of the copper(I) centres present a more or less regular CuS₂ (Cu1) or CuNS₂ (Cu2 and Cu5) triangular coordination geometry, whereas remaining three ones adopts a tetrahedral CuI₃S (Cu3 and Cu6) or CuI₂S₂ (Cu4) ones (Figure S3). The thiophenolate ligands maximize its coordination capabilities by bridging three (S1 and S2) and even four (S3) adjacent metal centres. The tetracoordination of a thiolate group is less common than the tricoordination but there are some examples in the literature.⁴⁸⁻⁵¹ The combination of both coordination modes generate a skeleton of fused non planar Cu₆S₆ rings that are reinforced by the presence of bridging iodides. Iodide anions I2 and I3 bridge three and two copper(I) metal centres in pyramidal and angular fashion, respectively. It helps generating a pseudo tubular structure in which the aromatic ring of the thiophenolate ligand and the methyl group of the acetonitrile ligands are decorating the outer surface of these tubes. The inner part of this tubular like structure is occupied by tetracoordinated iodide I1 which bridges four copper in a geometry that clearly lies in between the tetrahedral and square planar geometries. Finally, the acetonitrile ligand acts as terminal ligand completing the triangular coordination sphere of Cu2 and Cu5. All the copper(I) coordination bond distances are within their usual values for each type of donor atom. On the other hand, the presence of such a highly connected 1D complex entity imposes the presence of some short Cu...Cu distances (2.884 and 2.932 Å) that are not present in compound **2**. The 1D complex entities, that run along the crystallographic *c* axis, are surrounded by four other ones to provide the final 3D crystalline structure (Figure 1c). There is no evidence of the presence of any relevant

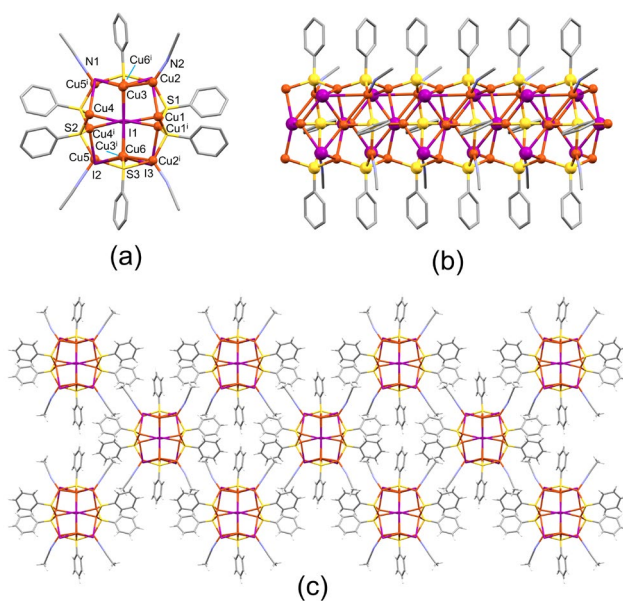


Fig. 2. View (a) along and (b) running along the *c*-axis of the 1D [Cu₆I₃(TP)₃(MeCN)₂]_n (**1**) chains and (c) their crystal packing.

supramolecular interaction apart from weak van der Waals forces.

Luminescent properties. In the last decades, Cu(I) complexes with thiolate ligands have been investigated for their optical properties.⁵²⁻⁵⁵ Among them, polynuclear complexes with phosphines as ancillary ligands represent one of the most studied family of compounds.⁵⁶⁻⁶⁰ The study of these systems by DFT theoretical calculations has allowed assigning the luminescence to transitions from triplet excited states which are mixed ($d \rightarrow s$) and LMCT (ligand to metal charge transfer).^{59, 61, 62} However, the optical properties of polymeric copper(I) thiolate compounds remain still little developed. We have recently reported the synthesis, structural characterization by X-ray diffraction analysis and study of their optical properties of the homoleptic copper(I) arylthiolates $[\text{Cu}(p\text{-SC}_6\text{H}_4\text{-R})]$ ($\text{R} = \text{COOH}, \text{COOMe}$).⁴⁷

Figure 4 displays the photoemission spectra of **1** and **2** upon excitation at 359 nm recorded at room temperature. Compound **1** shows blue emission with two peaks and maximum values centred at 417 and 469 nm and weak shoulders at 453, 484 and 495 nm. In addition, a very weak low energy emission band at 622 nm was also observed. Compound **2** presents intense red luminescence, with a strong peak at 645 nm. In that case, blue emission maxima at 417 and 470 nm with very low intensity were detected. Otherwise, free ligand thiophenol displays blue photoluminescent emission with maxima at 418 and 469 nm (Figure S4). The emission spectra of compounds **1** and **2** in the blue region are similar to the corresponding free ligand thiophenol, therefore this high energy emission can be ascribed as originating from intraligand (IL) $\pi\text{-}\pi^*$ transitions. Otherwise, taking into account previous studies on Cu(I) thiolates,^{47, 61, 62} the low energy emission can be assigned to ligand–metal charge transfer (LMCT). In order to try to establish a relationship between structure and optical properties, the structure of **2** is similar to the previously reported polymeric homoleptic copper(I) arylthiolates $[\text{Cu}(p\text{-SC}_6\text{H}_4\text{-R})]$ ($\text{R} = \text{COOH}, \text{COOMe}$)⁴⁷ and these compounds also shown a low energy band in red

region most probably arises from an $^3\text{LMCT}$ (modified by a contribution from $\text{Cu}\cdots\text{Cu}$ interactions).^{1, 61, 63} Although **1** shows a different structure to that of **2**, the similarity in the observed low energy bands for both compounds seems to indicate that is not very affected by the structure, being the presence of thiophenol ring the key factor that have influence. This observation is in line with the assignment of an emissive origin derived mainly from states of a LMCT ($\text{RS}^- \rightarrow \text{Cu}$) transition.

Electrical Conductivity and DFT Calculations. Electrical conductivity of compounds **1** and **2** has been measured at 25 °C, using direct current (DC) and two-contact method on pressed pellets of polycrystalline solids. Bulk electrical conductivity values of $1.2 \cdot 10^{-8} \text{ S cm}^{-1}$ and $3.7 \cdot 10^{-4} \text{ S cm}^{-1}$ respectively, were estimated from their corresponding current–voltage plot (ESI, Figures S5 and S6). These values indicate a moderate and good electrical conductivity, respectively for **1** and **2**, compared to that shown by other Cu(I) thiolate based electrically conductive coordination polymers^{16,35,36,64} and could suggest a semiconductor behaviour which will be supported by the theoretical calculations (see theoretical calculations below).

Compound **1** is a one-dimensional coordination polymer with four different environments for its copper atoms (Figure S3). The intricate structure of **1** makes difficult to rationalize its possible mechanism of conduction. As stated in its structural description, **1** presents of two types of chains throughout its structure, one based on S–Cu–S bonds and another on I–Cu–I bonds. These two chains could be the predominant pathways of electron mobility, counteracting their effectiveness (Figure 5a). The Cu–S (2.223–2.354 Å) and Cu–I (2.6927–3.129 Å) distances as well as the angles (Tables S1 and S2), could allow a sufficiently effective overlap between the copper d_{z^2} orbital and p orbitals of the sulfur and iodine atoms to produce moderate electrical conductivity ($1.2 \cdot 10^{-8} \text{ S cm}^{-1}$). The one-dimensional structure of compound **2** is much simpler (Figure 3). It is composed of a single flat trigonal environment for copper, which is bonded to three sulfur atoms, forming Cu_3S_3 rings, connected in turn by sulfurs. Although Cu–S distances (2.270–2.303 Å) and angles are similar to those found in compound **1** (Table S3 and S4), the smaller distance between the copper atom and the plane formed by the three sulfur atoms implies a greater planarity (0.031 Å) and, therefore, a more effective orbitals overlapping.³⁶

In order to rationalize from a theoretical point of view the electronic conductivity results obtained for the compounds **1** and **2**, we have carried out First-principles Density-functional-theory (DFT)-based calculations. In the theoretical simulations, we have used the atomic coordinates found in the X-ray structures of **1** and **2**, in order to evaluate the real geometry of the materials in the crystal phase in which the electrical measurements were carried out. In both compounds, the final residual forces acting on each atom in all the calculations were below 0.1 eV/\AA , which is low enough to guarantee perfectly converged and realistic results for such complex systems from a theoretical point of view. This noticeably good geometrical transferability between the experimental configurations and our theoretical implementation has already provided successful results for other similar polymer crystals.³⁵ The electronic

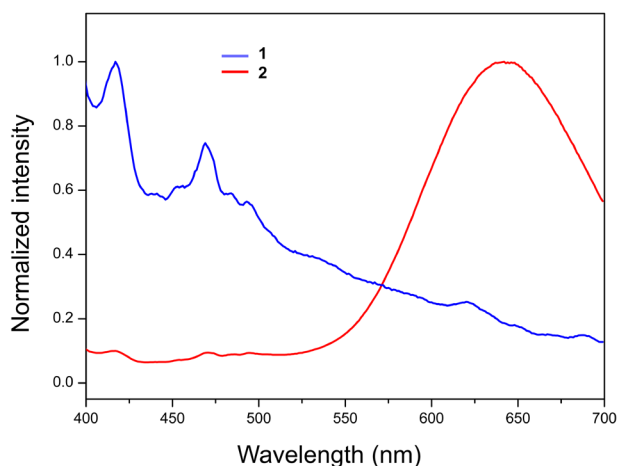


Fig. 4. Normalized emission spectra of **1** (blue) and **2** (red) in the solid state at room temperature. $\lambda_{\text{exc}} = 359 \text{ nm}$.

structure calculations yield minimum values of the transport gaps at Γ points of 1.98 and 1.67 eV for **1** and **2**, respectively (Figure 5b). Therefore, theory predicts all the compounds as classical wide band-gap semiconductors. Compound **1** shows a canonical n-type semiconducting character, with the Fermi level almost pinning into the conduction band; whilst compound **2** does not show a clear n or p-type semiconducting character, with the Fermi level located in the midgap region. Computed transport-gaps of 1.98 and 1.67 eV for **1** and **2**, respectively, are in excellent agreement with the measured electrical conductivity values of 1.2×10^{-8} and 3.7×10^{-4} S cm $^{-1}$. It is important to remark the fact that in both compounds **1** and **2** the conduction bands are electronically degenerated, showing

a degeneracy of 2 and 4, respectively. This high electronic degeneracy arises from their corresponding rotational symmetries. This fact has its reflection in the noticeable intensity of the DOS profile for the conduction bands of both compounds (w.r.t. the valence bands), and in the conductivity performance, since the conduction band can easily accommodate promoting carriers coming from the valence band by an external potential or an increasing temperature. This behaviour translates in the fact that a relatively wide transport gap such as 1.67 eV, in compound **2**, yields a conductivity value of 3.7×10^{-4} S cm $^{-1}$. Figure S7 shows the valence and conduction band orbital electron isodensities (with values of 10^{-4} e $^{-\text{\AA}^{-3}}$) for the compounds **1** and **2**. In this figure it is possible to appreciate that for compound **1** the valence electron isodensity is mostly located along the metal skeleton, whilst the conduction electron isodensity is mostly located on the organic ligands. Nevertheless, for the compound **2**, both valence and conduction bands show contributions from both the metallic scaffold and the organic ligands. This is translated in a slightly higher metal-ligand hybridization, which yields a lower transport gap and a higher conductivity for **2**. Additionally, in the Figure S7 we can also appreciate the emerging orbital symmetry, which leads to the electronic degeneracy of the conduction band aforementioned.

Experimental section

Materials and Methods

All the reagents were purchased from Sigma-Aldrich and used as received. FTIR spectra (KBr pellets) were recorded on a Perkin-Elmer 1650 spectrophotometer. C, H, N, S elemental analyses were performed by the Microanalysis Service of the Universidad Autónoma de Madrid on a Perkin-Elmer 240 B microanalyser. Powder X-ray diffraction experiments were carried out on a Diffractometer PANalyticalX'Pert PRO theta/2theta primary monochromator and detector with fast X'Celerator. The samples have been analysed with scanning theta/2theta. Direct current (DC) electrical conductivity measurements were performed on pressed pellets of polycrystalline solids of compounds **1** and **2**, with carbon paint at 300 K and two contacts. The contacts were made with wolfram wires (25 μ m diameter). The samples were measured at 300 K applying an electrical current with voltages from +10 to -10 V. Luminescence excitation and emission spectra of the solid compounds were performed at 25 °C using a 48000 s (T-Optics) spectrofluorometer from SLM-Aminco. A front face sample holder was used for data collection and oriented at 60° to minimize light scattering from the excitation beam on the cooled R-928 photomultiplier tube. Appropriate filters were used to eliminate Rayleigh and Raman scattering from the emission. Excitation and emission spectra were corrected for the wavelength dependence of the 450 W xenon arc excitation but not for the wavelength dependence of the detection system. Spectroscopic properties were measured by reflection (front face mode) on finely ground samples that were placed in quartz cells of 1 mm path length.

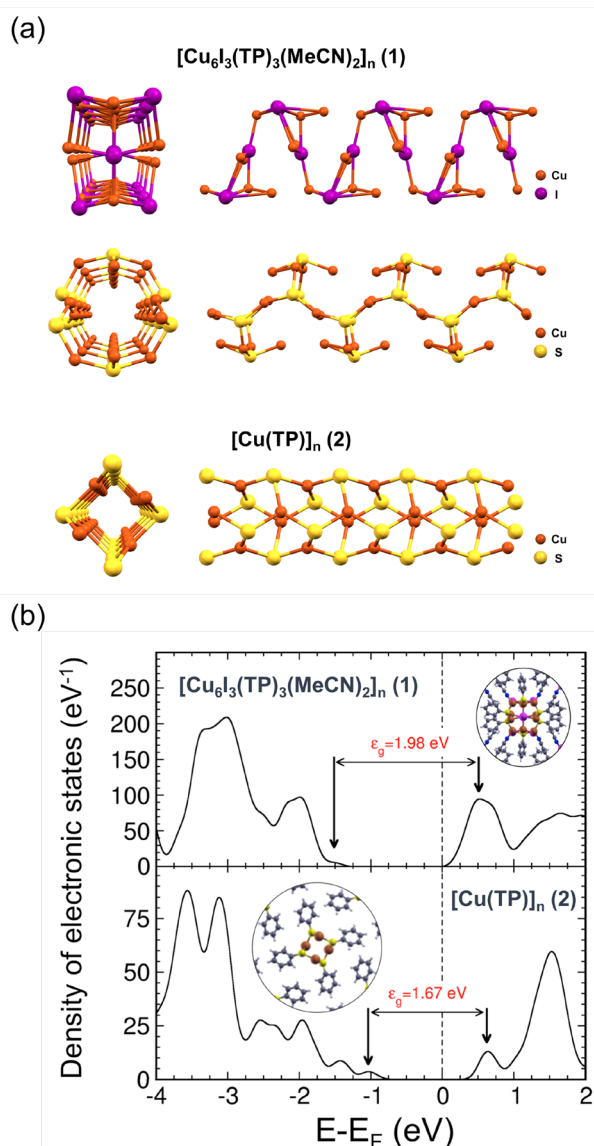


Fig. 5. a) Representation of the Cu-I and Cu-S substructures in **1** and Cu-S substructure in **2**. b) Computed total density of electronic states (in eV^{-1}) for compounds **1** (top panel) and **2** (bottom panel) as a function of the energy, referred to the Fermi level. Each energy level has been broadened by a Lorentzian profile with a line-width of 0.01 eV. Transport gap (ϵ_g) and geometries of each compound are also shown in each subpanel.

X-ray data collection and crystal structure determination. The X-ray diffraction data collections and structure determinations were done on a Bruker Kappa Apex II diffractometer using graphite-monochromated Mo-K α radiation ($\lambda=0.71073$ Å). The cell parameters were determined and refined by a least-squares fit of all reflections. A semi-empirical absorption correction (SADABS) was applied for all cases. All the structures were solved by direct methods using the SIR92 program⁶⁵ and refined by full-matrix least-squares on F^2 including all reflections (SHELXL97).⁶⁶ All calculations were performed using the WINGX crystallographic software package.⁶⁷ All non-hydrogen atoms were refined anisotropically. The hydrogen atoms were included in their calculated positions and refined riding on the respective parent atoms. Relevant data acquisition and refinement parameters are gathered in Table 1. The main bond lengths and angles for **1** and **2** are shown in Tables S1-S4 (CCDC 1566448 for **1**).

Table 1. Crystallographic data for compound **1**.

	1
Empirical formula	C ₂₂ H ₂₁ Cu ₆ I ₃ N ₂ S ₃
Formula weight	1171.53
T (K)	200(2)
Crystal system	Monoclinic
Space group	$P 2_1/c$
a (Å)	20.6948(9)
b (Å)	19.1425(7)
c (Å)	7.5103(2)
α (°)	--
β (°)	92.828(2)
γ (°)	--
V (Å ³)	2971.58(19)
Z	4
GOF ^a	1.014
R_{int}	0.0794
Final R indices	
$[I > 2\sigma(I)]$	
$R1^b$	0.0446
$wR2^c$	0.0864
All data	
$R1^b$	0.0956
$wR2^c$	0.0864
Largest peak/hole (e ⁻ Å ⁻³)	1.267/-0.997

^[a] $S = [\sum w(F_o^2 - F_c^2)^2 / (N_{obs} - N_{param})]^{1/2}$ ^[b] $R1 = \sum ||F_o| - |F_c|| / \sum |F_o|$; ^[c] $wR2 = [\sum w(F_o^2 - F_c^2)^2 / \sum wF_o^2]^{1/2}$; $w = 1/[\sigma^2(F_o^2) + (aP)^2 + b]$ where $P = (\max(F_o^2, 0) + 2 F_c^2)/3$ with $a = 0.0420$ (**1**) and $b = 5.3536$ (**1**).

Theoretical methodology. All the Density Functional Theory (DFT)-based calculations have been carried out by the accurate and efficient plane-wave code QUANTUM ESPRESSO.⁶⁸ Within this atomistic simulation package the Kohn-Sham equations are solved using a periodic super-cell geometry. The exchange-correlation (XC) effects have been accounted through the Generalized Gradient Approximation (GGA) within the Perdew-Burke-Ernzerhof (PBE) parameterization.⁶⁹ To model the ion-electron interaction in the H, C, O, S and Cu atoms we have used RabeRappeKaxirasJoannopoulos (RRKJ) ultra-soft pseudopotentials.^{70, 71} The Brillouin zone (BZ) has been sampled by means of a $[6 \times 6 \times 1]$ Monkhorst-Pack grid⁷² (where the Cartesian XY plane corresponds here to the laminar plane) for **1**

and **2**. The one-electron wave-functions have been expanded in a basis of plane-waves with energy cut-offs of 400 and 500 eV for the kinetic energy and for the electronic density, respectively, which have been adjusted to achieve enough accuracy to guarantee a full convergence in energy and density.

Synthesis of [Cu₆I₃(TP)₃(MeCN)₂]_n (1**).** A solution of CuI (0.320 g, 1.65 mmol) in 12 mL of acetonitrile was added to a suspension of [Cu(TP)]_n (**2**) (0.070 g, 0.40 mmol) in 2 mL of the same solvent. The resultant mixture was stirred for one night at room temperature. Then, the grey precipitate formed was filtered and washed with a solution of CuI (0.175 g, 0.90 mmol) in 8 mL of acetonitrile (4 x 2 mL) and diethyl ether (2 x 2 mL) and then dried in air (0.063 g, 80 % yield based on Cu). Anal. calcd (%) for C₂₂H₂₁Cu₆I₃N₂S₃: C, 22.55; H, 1.81; N, 2.39; S, 8.21. Found (%): C, 22.58; H, 1.92; N, 2.31; S, 8.15. IR (KBr, cm⁻¹): 3043 (m), 2920 (m), 2305 (w), 2272 (w), 1576 (s), 1475 (s), 1435 (s), 1080(m), 1022 (m), 742 (s), 688 (s). The purity of the product was checked by X-ray powder diffraction (Figure S8). Single crystals of **1** suitable for X-ray diffraction were synthesized by heating a mixture of CuI (0.582 g, 3.00 mmol) and thiophenol (0.085 g, 0.75 mmol) in 5 mL of acetonitrile at 160 °C for 72 h. The resulting yellow solution was filtered off to separate the unreacted CuI and was allowed to stand in a refrigerator for one week.

Synthesis of [Cu(TP)]_n (2**).** A mixture of Cu(BF₄)₂·xH₂O (0.383 g, 1.50 mmol) and thiophenol (0.341 g, 3.00 mmol) in 12 mL of ethanol was placed in a 70 mL Teflon-lined vessel, sealed and sited into a microwave oven equipped with a rotor. The multimode microwave has a twin magnetron (2 x 800 W, 2.45GHz) with a maximum delivered power of 1000 W. The temperature was increased from room temperature to 120 °C in 10 min (microwave power was set at 350 W) and kept for 1 h. Then, the vessel was slowly cooled down to room temperature. A yellow solid was obtained, washed with ethanol and diethyl ether, and then dried in a vacuum at 60 °C for 4 h (0.161 g, 62 % yield based on Cu). Anal. calcd (%) for C₆H₅CuS: C, 41.72; H, 2.92; S, 18.57. Found (%): C, 41.45; H, 2.99; S, 18.38. IR (KBr, cm⁻¹): 3062 (w), 1577 (s), 1473 (s), 1437 (m), 1080 (m), 1024 (m), 729 (s), 685 (s). The purity of the product was checked by X-ray powder diffraction (Figure S9). Our attempts to obtain single crystals of **2** were unsuccessful.

Conclusions

In this work, we show that the direct self-assembly of CuI with thiophenol produces two different 1D coordination polymers with interesting multifunctional properties, *i.e.* semiconductivity and luminescence. Interestingly, we have found that the ratio of CuI in acetonitrile is the key factor determining the reversible conversion between **1** and **2** under ambient conditions.

These 1D-CPs display high and low energy luminescence emission in the solid state, which can be assigned to LMCT transition involving the thiophenolate ligand. Moreover, their electrical characterization reveals a semiconductor behaviour at room temperature. Theoretical calculations have been used to rationalize these findings.

Conflicts of interest

There are no conflicts to declare.

Acknowledgements

This work was supported in part by MICINN (grant MAT2016-77608-C3-1-P).

References

- 1 V. W.-W. Yam and K. K. Lo, *Chem. Soc. Rev.*, 1999, **28**, 323.
- 2 V. W.-W. Yam, W. Kit-Mai Fung and K.-K. Cheung, *Chem. Commun.*, 1997, 963.
- 3 V. W.-W. Yam and K. M.-C. Wong, *Chem. Commun.*, 2011, **47**, 11579.
- 4 E. Cariati, E. Lucenti, C. Botta, U. Giovannella, D. Marinotto and S. Righetto, *Coord. Chem. Rev.*, 2016, **306**, 566.
- 5 R. D. Costa, D. Tordera, E. Orti, H. J. Bolink, J. Schonle, S. Graber, C. E. Housecroft, E. C. Constable and J. A. Zampese, *J. Mater. Chem.*, 2011, **21**, 16108.
- 6 P. J. Walsh, N. J. Lundin, K. C. Gordon, J.-Y. Kim and C.-H. Lee, *Opt. Mater.*, 2009, **31**, 1525.
- 7 M. J. Leidl, F.-R. Kuchle, H. A. Mayer, L. Wesemann and H. Yersin, *J. Phys. Chem. A*, 2013, **117**, 11823.
- 8 F. Dumur, *Org. Electron.*, 2015, **21**, 27.
- 9 Z. Liu, J. Qiu, F. Wei, J. Wang, X. Liu, M. G. Helander, S. Rodney, Z. Wang, Z. Bian, Z. Lu, M. E. Thompson and C. Huang, *Chem. Mater.*, 2014, **26**, 2368.
- 10 M. J. Leidl, D. M. Zink, A. Schinabeck, T. Baumann, D. Volz and H. Yersin, *Top. Curr. Chem.*, 2016, **374**, 25.
- 11 K. Tsuge, Y. Chishina, H. Hashiguchi, Y. Sasaki, M. Kato, S. Ishizaka and N. Kitamura, *Coord. Chem. Rev.*, 2016, **306**, 636.
- 12 R. Peng, M. Li and D. Li, *Coord. Chem. Rev.*, 2010, **254**, 1.
- 13 C. H. Arnby, S. Jagner and I. Dance, *CrystEngComm*, 2004, **6**, 257.
- 14 Y. Chen, H.-X. Li, D. Liu, L.-L. Liu, N.-Y. Li, H.-Y. Ye, Y. Zhang and J.-P. Lang, *Cryst. Growth Des.*, 2008, **8**, 3810.
- 15 B.-C. Tzeng and T.-Y. Chang, *Cryst. Growth Des.*, 2009, **9**, 5343.
- 16 Y. Chen, Z.-O. Wang, Z.-G. Ren, H.-X. Li, D.-X. Li, D. Liu, Y. Zhang and J.-P. Lang, *Cryst. Growth Des.*, 2009, **9**, 4963.
- 17 Z. Fu, J. Lin, L. Wang, C. Li, W. Yan and T. Wu, *Cryst. Growth Des.*, 2016, **16**, 2322.
- 18 G. Kang, Y. Jeon, K. Y. Lee, J. Kim and T. H. Kim, *Cryst. Growth Des.*, 2015, **15**, 5183.
- 19 T. Hayashi, A. Kobayashi, H. Ohara, M. Yoshida, T. Matsumoto, H.-C. Chang and M. Kato, *Inorg. Chem.*, 2015, **54**, 8905.
- 20 P. D. Harvey and M. Knorr, *Macromol. Rapid Commun.*, 2010, **31**, 808.
- 21 M. Knorr, F. Guyon, A. Khatyr, C. Strohmman, M. Allain, S. M. Aly, A. Lapprand, D. Fortin and P. D. Harvey, *Inorg. Chem.*, 2012, **51**, 9917.
- 22 J. Conesa-Egea, F. Zamora and P. Amo-Ochoa, *Coord. Chem. Rev.*, 2019, **381**, 65.
- 23 M. Knorr, A. Khatyr, A. Dini Aleo, A. El Yaagoubi, C. Strohmman, M. M. Kubicki, Y. Rousselin, S. M. Aly, D. Fortin, A. Lapprand and P. D. Harvey, *Cryst. Growth Des.*, 2014, **14**, 5373.
- 24 K. M. Henline, C. Wang, R. D. Pike, J. C. Ahern, B. Sousa, H. H. Patterson, A. T. Kerr and C. L. Cahill, *Cryst. Growth Des.*, 2014, **14**, 1449.
- 25 D. Coucouvanis, C. N. Murphy and S. K. Kanodia, *Inorg. Chem.*, 1980, **19**, 2993.
- 26 H. J. Schugar, C.-C. Ou, J. A. Thich, J. A. Potenza, T. R. Felthouse, M. S. Haddad, D. N. Hendrickson, W. Furey and R. A. Lalancette, *Inorg. Chem.*, 1980, **19**, 543.
- 27 O. Veselska and A. Demessence, *Coord. Chem. Rev.*, 2018, **355**, 240.
- 28 E. Neofotistou, C. D. Malliakas and P. N. Trikalitis, *Inorg. Chem.*, 2007, **46**, 8487.
- 29 S. S. Alexandre, J. M. Soler, P. J. Sanz Miguel, R. W. Nunes, F. Yndurain, J. Gómez-Herrero and F. Zamora, *Appl. Phys. Lett.*, 2007, **90**, 193107.
- 30 S. Delgado, P. J. Sanz Miguel, J. L. Priego, R. Jiménez-Aparicio, C. J. Gómez-García and F. Zamora, *Inorg. Chem.*, 2008, **47**, 9128.
- 31 G. Givaja, P. Amo-Ochoa, C. J. Gómez-García and F. Zamora, *Chem. Soc. Rev.*, 2012, **41**, 115.
- 32 C.-M. Che, C.-H. Li, S. S.-Y. Chui, V. A. L. Roy and K.-H. Low, *Chem. Eur. J.*, 2008, **14**, 2965.
- 33 X. Huang, P. Sheng, Z. Tu, F. Zhang, J. Wang, H. Geng, Y. Zou, C.-a. Di, Y. Yi, Y. Sun, W. Xu and D. Zhu, *Nat. Commun.*, 2015, **6**, 7408.
- 34 J. Troyano, E. Zapata, J. Perles, P. Amo-Ochoa, V. Fernández-Moreira, J. I. Martínez, F. Zamora and S. Delgado, *Inorg. Chem.*, 2019, **58**, 3290.
- 35 J. Troyano, J. Perles, P. Amo-Ochoa, J. I. Martínez, M. Gimeno, V. Fernández-Moreira, F. Zamora and S. Delgado, *Chem. Eur. J.*, 2016, **22**, 18027.
- 36 J. Troyano, Ó. Castillo, P. Amo-Ochoa, V. Fernández-Moreira, C. J. Gómez-García, F. Zamora and S. Delgado, *J. Mater. Chem. C*, 2016, **4**, 8545.
- 37 C. Janiak, *Dalton Trans.*, 2003, 2781.
- 38 in *Coordination Polymers: Design, Analysis and Application*, The Royal Society of Chemistry, 2009, pp. 1-18.
- 39 J.-J. Zhang, Y. Zhao, S. A. Gamboa, M. Muñoz and A. Lachgar, *Eur. J. Inorg. Chem.*, 2008, **2008**, 2982.
- 40 J.-J. Wu, Y.-X. Ye, Y.-Y. Qiu, Z.-P. Qiao, M.-L. Cao and B.-H. Ye, *Inorg. Chem.*, 2013, **52**, 6450.
- 41 Y. Kataoka, N. Yano, T. Shimodaira, Y.-N. Yan, M. Yamasaki, H. Tanaka, K. Omata, T. Kawamoto and M. Handa, *Eur. J. Inorg. Chem.*, 2016, **2016**, 2810.
- 42 X. Cui, A. N. Khlobystov, X. Chen, D. H. Marsh, A. J. Blake, W. Lewis, N. R. Champness, C. J. Roberts and M. Schröder, *Chem. Eur. J.*, 2009, **15**, 8861.
- 43 A. N. Khlobystov, N. R. Champness, C. J. Roberts, S. J. B. Tandler, C. Thompson and M. Schroder, *CrystEngComm*, 2002, **4**, 426.
- 44 C. Thompson, N. R. Champness, A. N. Khlobystov, C. J. Roberts, M. Schröder, S. J. B. Tandler and M. J. Wilkinson, *J. Microsc.*, 2004, **214**, 261.
- 45 J.-J. Zhang, C. S. Day and A. Lachgar, *CrystEngComm*, 2011, **13**, 133.
- 46 J. Troyano, J. Perles, P. Amo-Ochoa, J. I. Martinez, F. Zamora and S. Delgado, *CrystEngComm*, 2014, **16**, 8224.
- 47 J. Troyano, O. Castillo, J. I. Martínez, V. Fernández-Moreira, Y. Ballesteros, D. MasPOCH, F. Zamora and S. Delgado, *Adv. Funct. Mater.*, 2018, **28**, 1704040.
- 48 L. Fernandez-Recio, D. Fenske and O. Fuhr, *Z. Anorg. Allg. Química*, 2008, **634**, 2853.
- 49 O. Kluge, K. Grummt, R. Biedermann and H. Krautscheid, *Inorg. Chem.*, 2011, **50**, 4742.
- 50 O. Fuhr, L. Fernandez-Recio and D. Fenske, *Eur. J. Inorg. Chem.*, 2005, **2005**, 2306.
- 51 G. Gupta and S. Bhattacharya, *RSC Adv.*, 2015, **5**, 94486.
- 52 M. Osawa, *Chem. Commun.*, 2014, **50**, 180.
- 53 D. M. Knotter, G. Blasse, J. P. M. Van Vliet and G. Van Koten, *Inorg. Chem.*, 1992, **31**, 2196.
- 54 D. M. Knotter, G. van Koten, H. L. van Maanen, D. M. Grove and A. L. Spek, *Angew. Chem. Int. Ed.*, 1989, **28**, 341.
- 55 M. Baumgartner, H. Schmalle and E. Dubler, *Polyhedron*, 1990, **9**, 1155.
- 56 A. Eichhöfer, G. Buth, S. Lebedkin, M. Kühn and F. Weigend, *Inorg. Chem.*, 2015, **54**, 9413.

- 57 P. C. Ford, E. Cariati and J. Bourassa, *Chem. Rev.*, 1999, **99**, 3625.
- 58 P. A. Papanikolaou, A. G. Papadopoulos, E. G. Andreadou, A. Hatzidimitriou, P. J. Cox, A. A. Pantazaki and P. Aslanidis, *New J. Chem.*, 2015, **39**, 4830.
- 59 R. Langer, M. Yadav, B. Weinert, D. Fenske and O. Fuhr, *Eur. J. Inorg. Chem.*, 2013, **21**, 3623.
- 60 B. Hu, C.-Y. Su, D. Fenske and O. Fuhr, *Inorg. Chim. Acta*, 2014, **419**, 118.
- 61 F. Sabin, C. K. Ryu, P. C. Ford and A. Vogler, *Inorg. Chem.*, 1992, **31**, 1941.
- 62 V. W.-W. Yam, K. K.-W. Lo, C.-R. Wang and K.-K. Cheung, *J. Phys. Chem. A*, 1997, **101**, 4666.
- 63 V. W.-W. Yam, C.-H. Lam, W. K.-M. Fung and K.-K. Cheung, *Inorg. Chem.*, 2001, **40**, 3435.
- 64 Y. Zhang, T. Xia, K. M. Yu, F. Zhang, H. Yang, B. Liu, Y. An, Y. Yin and X. Chen, *ChemPlusChem*, 2014, **79**, 559.
- 65 A. Altomare, G. Casciarano, C. Giacovazzo and A. Guagliardi, *J. Appl. Cryst.*, 1993, **26**, 343.
- 66 G. M. Sheldrick, SHELXL-97, Program for Crystal Structure Refinement; Universität Göttingen., 1997.
- 67 L. Farrugia, *J. Appl. Cryst.*, 1999, **32**, 837.
- 68 G. Paolo, B. Stefano, B. Nicola, C. Matteo, C. Roberto, C. Carlo, C. Davide, L. C. Guido, C. Matteo, D. Ismaila, C. Andrea Dal, G. Stefano de, F. Stefano, F. Guido, G. Ralph, G. Uwe, G. Christos, K. Anton, L. Michele, M.-S. Layla, M. Nicola, M. Francesco, M. Riccardo, P. Stefano, P. Alfredo, P. Lorenzo, S. Carlo, S. Sandro, S. Gabriele, P. S. Ari, S. Alexander, U. Paolo and M. W. Renata, *J. Phys. Condens. Matter.*, 2009, **21**, 395502.
- 69 J. P. Perdew, K. Burke and M. Ernzerhof, *Phys. Rev. Lett.*, 1997, **78**, 1396.
- 70 A. M. Rappe, K. M. Rabe, E. Kaxiras and J. D. Joannopoulos, *Phys. Rev. B*, 1990, **41**, 1227.
- 71 N. Mounet and N. Marzari, *Phys. Rev. B*, 2005, **71**, 205214.
- 72 D. J. Chadi and M. L. Cohen, *Phys. Rev. B*, 1973, **8**, 5747.